

# NUMERICAL INVESTIGATION OF FLUID FLOW AND HEAT TRANSFER CHARACTERISTICS IN SINE, TRIANGULAR, AND ARC-SHAPED CHANNELS

by

**Mohammad Zakir HOSSAIN and  
Abdul Kalam Mohammad SADRUL ISLAM**

Original scientific paper  
UDC: 532.54:519.876.5:536.24  
BIBLID: 0354-9836, 11 (2007), 1, 17-26

*Time dependent Navier-Stokes and energy equations have been solved to investigate the fluid flow and heat transfer characteristics in wavy channels. Three different types of two dimensional wavy geometries (e. g. sine-shaped, triangular, and arc-shaped) are considered. All of them are of single wave and have same geometric dimensions. Periodic boundary conditions are used to attain fully developed flow. The flow in the channels has been observed to be steady up to a critical Reynolds number, which depends on the geometric configuration. Beyond the critical Reynolds number a self-sustained oscillatory flow has been observed. As a result of this oscillation, there is increased mixing between core and the near-wall fluids, thereby increasing the heat transfer rate. For the same geometric dimensions, flow becomes unsteady at relatively lower Reynolds number in the arc-shaped channel.*

Key words: *numerical solution, fluid flow, heat transfer, wavy channel, oscillatory flow*

## Introduction

For well over a century, efforts have been made to produce more efficient heat exchangers by employing various methods of heat transfer augmentation. The study of enhanced heat transfer has gained serious momentum during recent years due to increased demands by industry for heat exchange equipment that is less expensive to build and operate. Savings in materials and energy use also provide strong motivation for the development of improved methods of enhancement. When designing heat exchangers for air conditioning and refrigeration applications, it is imperative that they are made as compact and lightweight as possible. This is especially true for cooling systems in automobiles and spacecrafts, where volume and weight constraints are particularly important.

The wavy passage is a special surface that can be used to promote heat transfer. This is accomplished due to complex recirculatory flows and boundary layer separation. Nishimura *et al.* [1] investigated flow characteristics such as flow pattern, pressure drop, and wall shear stress in a channel with symmetric sinusoidal wavy wall. This study re-

ported that at Reynolds number greater than 700, turbulent flow occurred owing to the onset of unsteady vortex motion. Sparrow *et. al.* [2, 3] presented the effect of inlet condition, inter wall spacing and protruding edge on fluid flow and heat transfer. Vanka *et. al.* [4, 5] have presented numerical results on developing flow and heat transfer characteristics in a furrowed wavy channel. They found that at low Reynolds numbers, the flow in the wavy passage was steady, characterized by steady separation bubbles in the troughs of the waves. However, as the Reynolds number is increased beyond a modest value, the flow becomes unsteady, with the rolling up of the shear layers on the channel walls. When the flow becomes unsteady, there is increased mixing between the core and near-wall fluids, resulting in enhanced heat transfer rates and pressure drops. Niceno and Nobile [6] investigated the fluid flow and heat transfer characteristics in sinusoidal and arc-shaped channels numerically through a time-accurate, unstructured covolume method. They found that the friction factors for both channels were consistently higher than that of the parallel-plate channels, and heat transfer rates increase in unsteady regimes.

Computations for fully developed flow are less troublesome, because periodic boundary conditions allow the computational domain to be reduced to a single wavelength. Here, the fully developed flow calculations are used to expand the space parameters under consideration. Three different geometries (sine-shaped, triangular, and arc-shaped) of the wavy passage are chosen, and their effects on flow and heat transfer behavior are observed.

### Problem formulation

The governing equations for unsteady, incompressible and laminar flow are:

$$\frac{\partial u}{\partial x} + \frac{\partial v}{\partial y} = 0 \quad (1)$$

$$\frac{\partial u}{\partial t} + u \frac{\partial u}{\partial x} + v \frac{\partial u}{\partial y} = \frac{1}{\rho} \frac{\partial p}{\partial x} - \frac{\mu}{\rho} \left( \frac{\partial^2 u}{\partial x^2} + \frac{\partial^2 u}{\partial y^2} \right) \quad (2)$$

$$\frac{\partial v}{\partial t} + u \frac{\partial v}{\partial x} + v \frac{\partial v}{\partial y} = \frac{1}{\rho} \frac{\partial p}{\partial y} - \frac{\mu}{\rho} \left( \frac{\partial^2 v}{\partial x^2} + \frac{\partial^2 v}{\partial y^2} \right) \quad (3)$$

$$\frac{\partial \theta}{\partial t} + u \frac{\partial \theta}{\partial x} + v \frac{\partial \theta}{\partial y} = \frac{1}{\alpha} \left( \frac{\partial^2 \theta}{\partial x^2} + \frac{\partial^2 \theta}{\partial y^2} \right) \quad (4)$$

The dimensionless temperature  $\theta$  is defined as,  $\theta = (T - T_w)/(T_{\text{bin}} - T_w)$  where  $T_w$  is the temperature prescribed uniformly along the wall, and  $T_{\text{bin}}$  the bulk mean temperature evaluated at the inlet section of the computational domain.

## Geometry

All the geometries considered in this study are shown in fig. 1. The dimensions of each of the channels are chosen to correspond exactly with those used in the experiments of Nishimura, *et. al* [1], as well as several subsequent experimental and numerical studies. The channels consist of two curved wavy walls that are arranged with a mean spacing ( $H_{avg}$ ) of 1.3 dimensionless units. Each wave has a minimum height ( $H_{min}$ ) of 0.6 units, a maximum height ( $H_{max}$ ) of 2.0 units and the amplitude ( $a$ ) of the sinusoidal walls is 0.35 units. Each periodic wavelength ( $\lambda$ ) spans 2.8 units in the stream wise direction.

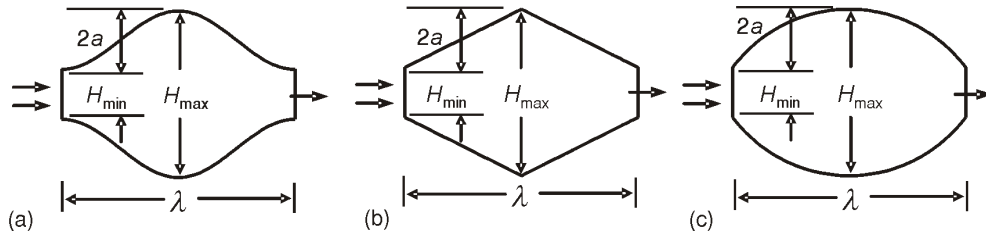


**Figure 1. Geometric configurations of (a) sinusoidal, (b) triangular, and (c) arc-shaped channel**

## Boundary conditions

Along the walls of the channels, no-slip boundary conditions are prescribed for the Cartesian velocities, along with a constant isothermal temperature distribution *i. e.:*  $u_w = 0$ ,  $v_w = 0$ , and  $\theta_w = 1$ .

For the pressure equation, no boundary conditions are necessary at the walls since the cell face fluxes are known (to be zero) directly. A uniform velocity is prescribed at the inlet. To attain the fully developed flow in the stream wise direction, the following periodic boundary conditions are used for a wave of length  $\lambda$ :

$$u(0, y, t) = u(\lambda, y, t) \quad v(0, y, t) = v(\lambda, y, t) \quad \theta(0, y, t) = \theta(\lambda, y, t) \quad (5)$$

The above boundary conditions in eqs. (5) are enforced by simply swapping values between the inflow and outflow boundaries.

## Numerical solution

In this study, the standard Finite Volume (FV) method is used. The FV method starts from the conservation equation in integral form. The integral forms of governing equations are discretized using control volume based FV method [7]. The solution do-

main is first subdivided into a finite number of contiguous control volumes (CVs), and the conservation equations are applied to each CV. At the centroid of each CV lies a computational node at which the variable values are to be calculated. Collocated arrangement is used for all variables, *i. e.* all variables are calculated at the same CV center. The final discretized forms of governing equations are solved iteratively using TDMA solver. Time integration is done using three time level method [7]. Iteration is continued until difference between two consecutive field values of variables is less than or equal to  $10^{-5}$ . For further stabilization of numerical algorithm, under-relaxation factors of 0.4-0.7 for  $u$ ,  $v$ , and  $T$ , and of 0.1-0.2 for  $p$  are used. A time step of 0.001 units is used for all of the flow calculations. A numerical velocity probe is arbitrarily placed at a height of  $0.75 H_{\max}$  in the tallest part of each of the geometry in order to monitor the fluctuations in the flow throughout the domain. Time signals of the fluctuations of  $u$ -velocities are monitored at the probe location. Time signals are also generated for the average friction factor and Nusselt numbers across the wave. These values are integrated to produce time-averaged quantities, which are indication of the average dimensionless heat transfer and pressure drop across each wave of the passage. All calculations are performed using a non-orthogonal curvilinear body fitted grid containing  $64 \times 64$  internal cells. A grid independence test is performed using  $32 \times 32$ ,  $48 \times 48$ , and  $64 \times 64$  grids [8]. All simulations are performed using Pentium III PC. A single simulation takes up to 8 hours of real time for 500 time steps for  $64 \times 64$  grids.

## Results and discussion

For sine-shaped wavy channel, it has been observed that the flow become unsteady around  $Re = 205$ . Before this  $Re$ , the streamline plot shows single trapped vortices in the cavities and almost perfectly straight core flow (fig. 2). This is the expected pattern for steady flow in a wavy channel [5]. At  $Re = 300$ , the time signal of  $u$ -velocity (fig. 3) represents a sinusoidal function corresponding to the self-sustained oscillatory flow. The growth of the instabilities is saturated by nonlinearities and the flow settles into a time-periodic, self-sustained oscillatory flow with one fundamental frequency of 20 with some of its harmonics as it is shown by the Fast Fourier Transform (FFT) analysis of the  $u$ -velocity. An unsteady streamline plot at  $Re = 300$  for the unsteady flow in the sinusoidal channel is given in fig. 4. The specific pattern varies with time, but the unsteady flow

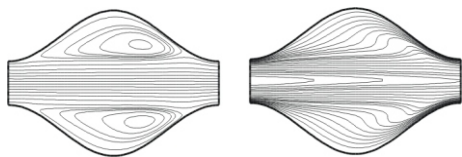


**Figure 2. Instantaneous streamline plot (left) and isotherm (right) for sine-shaped channel at  $Re = 180$**

always produces increased mixing and heat transfer rates. This can be seen in fig. 5. For steady flow, the Nusselt numbers vary very little with Reynolds number. Once the flow becomes unsteady, Nusselt number increases rapidly with Reynolds number. Figure 5 also shows the time averaged friction factor at various  $Re$  for both steady and unsteady flow in the sinusoidal channel. After slight increase in friction factor when the

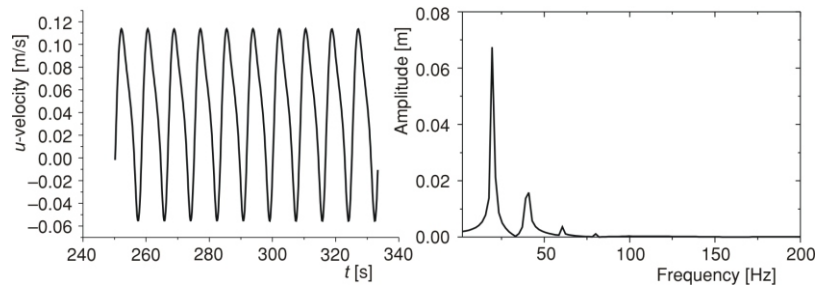


**Figure 3. Time signal of  $u$ -velocity at  $Re = 300$  for sine-shaped channel (left) and corresponding FFT (right)**

flow first becomes unsteady, time averaged friction factor continues to decrease with  $Re$ . However, the rate of this decrease slows down as  $Re$  is increased. Hence, there comes a point where the increasing  $Re$  renders diminishing benefits in heat transfer performance. The optimal value of  $Re$  depends on the specific criteria for evaluating performance, and on the dimensions of the passage. But it is known that wavy passages generally offer the best enhancement in the transitional regime.

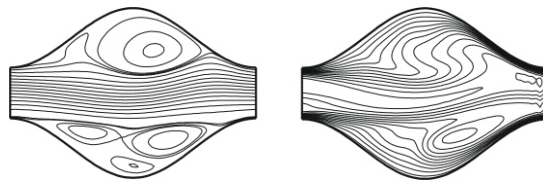


**Figure 4. Instantaneous streamline plot (left) and isotherm (right) for sine-shaped channel at  $Re = 300$**

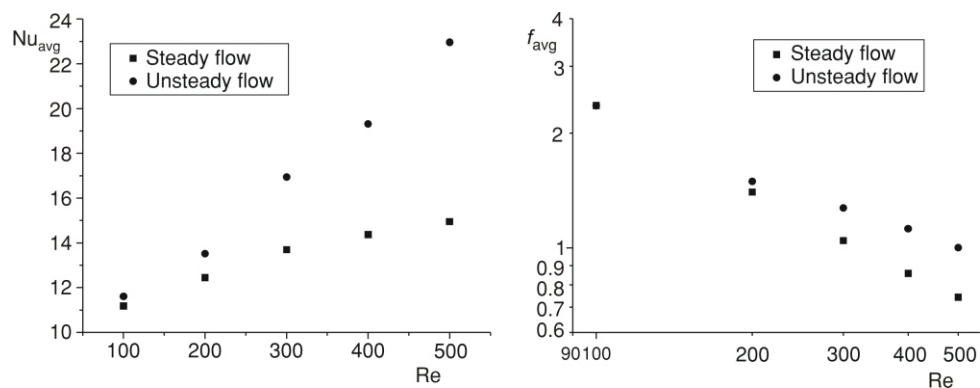


**Figure 5. Time averaged Nusselt number (left) and friction factor (right) for sine-shaped channel at various  $Re$**

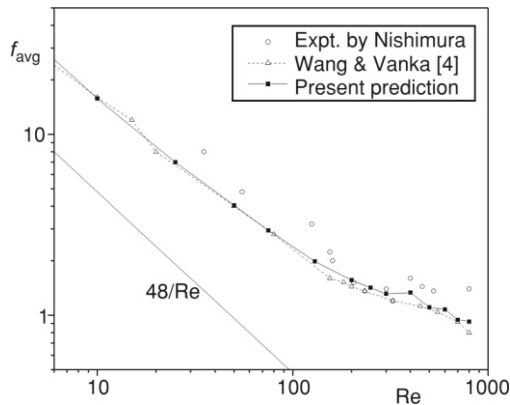


**Figure 6. Comparison of present predicted average friction factor with Nishimura *et al.* [1] and Wang & Vanka [4] for sine-shaped channel**

A comparison of the time mean friction factor averaged over the wave length is shown in fig. 6 for sine-shaped channel. The present prediction slightly under predicts the experimental data of Nishimura *et al.* [1] but shows a good agreement with the predicted values of Wang & Vanka [4]. In the steady regime the friction factor is approximately twice that of the planer channel. In the unsteady regime the friction factor is even more.

For triangular channel, it has been observed that the flow becomes unsteady around  $Re = 130$  *i. e.* flow becomes unsteady earlier than that of sine-shaped channel. Figure 7 shows the time evolution of  $u$ -velocity at the probe height for the triangular channel and the

corresponding FFT analysis at  $Re = 200$ . At this Reynolds number it represents a sinusoidal function corresponding to the self-sustained oscillatory flow as in the sine-shaped channel, but it has a higher frequency of fluctuation though the Reynolds number is low. The fundamental frequency of 52 Hz as it is shown by the FFT analysis of the  $u$ -velocity, is quite high and more dominant. Corresponding instantaneous streamline and isotherm plots are shown in fig. 8. Isotherm plot shows little mixing of core and near wall fluids.

Time averaged friction factor and Nusselt number for triangular channel changing with Reynolds number are shown in fig. 9. In this figure comparisons with corresponding sine-shaped channel are done as well. It has been observed that friction factor decreases

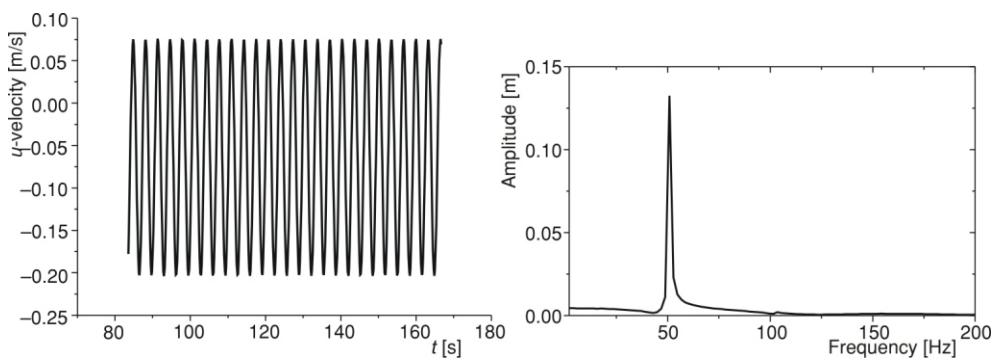


**Figure 7. Time signal of  $u$ -velocity at  $Re = 200$  for triangular channel (left) and corresponding FFT (right)**

with increase in  $Re$  in the case of sine-shaped channel, but in case of triangular channel up to around  $Re = 200$ , it decreases and afterwards it starts increasing with increase in  $Re$ . Values of friction factor and Nusselt number are lower than for the sine-shaped channel up to around  $Re = 200$ , after that both increase with increase in  $Re$ . It

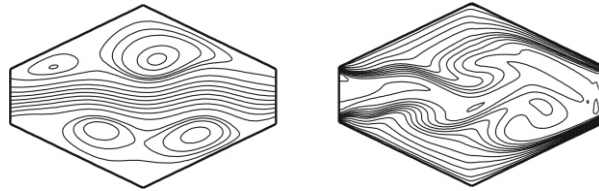


**Figure 8. Instantaneous streamline plot (left) and isotherm (right) for triangular channel at  $Re = 200$**

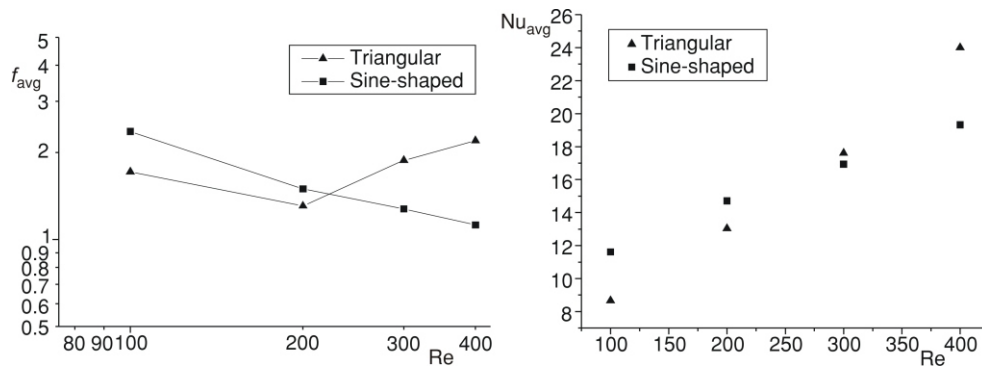


**Figure 9. Time averaged friction factor (left) and Nusselt number (right) for triangular channel at various  $Re$ ; comparison with sine-shaped channel**

has been observed that unsteadiness starts earlier in triangular channel than in the sine-shaped channel, and at  $Re=200$ , there occurs no unsteadiness in the sine-shaped channel. Due to unsteadiness, more molecular interactions occur which may result in increased heat transfer and friction factor. Here the values are reported up to  $Re = 400$ , as beyond these  $Re$  solutions of the governing equations become divergent.

For arc-shaped channel, it has been observed that the flow becomes unsteady at around  $Re = 80$  *i. e.* flow becomes unsteady earlier than that of both sine-shaped and triangular channels. Figure 10 shows the time evolution of the  $u$ -velocity at the probe height for the arc-channel and the corresponding FFT analysis at  $Re = 100$ . At this Reynolds number it represents a sinusoidal function corresponding to the self-sustained oscillatory flow, but the amplitudes of oscillations are varied as well. The FFT analysis shows that fundamental frequency is 61 Hz, which is quite high and dominant. Corresponding instantaneous streamline and isotherm plots are shown in fig. 11. The streamline plot shows

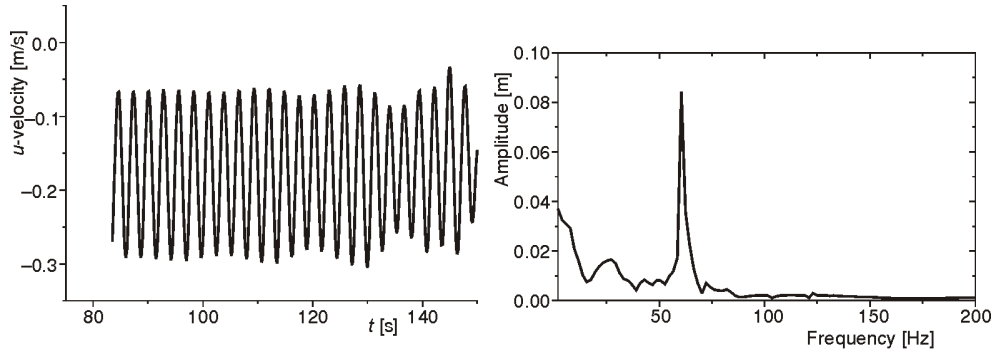


**Figure 10. Time signal of  $u$ -velocity at  $Re = 100$  for arc-channel (left) and corresponding FFT (right)**

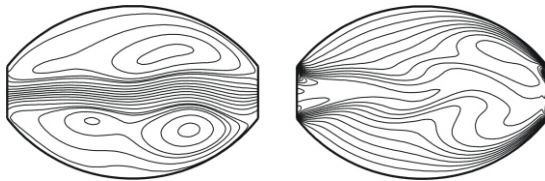


**Figure 11. Instantaneous streamline plot (left) and isotherm (right) for triangular channel at  $Re = 100$**

little unsteady vortices at the two furrows, and isotherm plot shows little mixing of core and near wall fluids.

Time averaged friction factor and Nusselt number for arc-shaped channel changing with Reynolds number are shown in fig. 12. Here the values are reported up to  $Re = 100$ , as beyond these  $Re$  solutions of the governing equations become divergent.

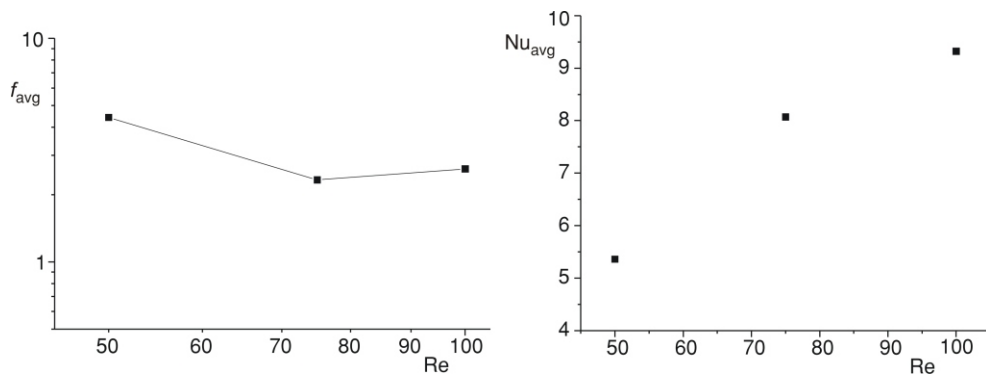


**Figure 12. Time averaged friction factor (left) and Nusselt number (right) for arc-channel at various  $Re$**



## Conclusions

Three different geometries (sine-shaped, triangular, and arc-shaped) of the wavy passages are chosen, and their effects on flow and heat transfer behaviors are observed. Among them for the same geometric dimensions, in the arc-shaped channel transition starts earlier *i. e.* at relatively low Reynolds number, for the sine-shaped channel, it is relatively high, and for triangular channel, it is in between two. Solutions for arc and triangular channels become divergent after certain Reynolds number as some recirculation and back flow occur at the outlet, which change the boundary conditions and it is not possible to handle with the code used. The FFT analyses show that the fundamental frequency of the self-sustained oscillation of arc-channel is quite high.

## Acknowledgment

The paper is an outcome of M. Sc. Eng. thesis work done by the first author at Department of Mechanical Engineering, Bangladesh University of Engineering & Technology (BUET). The authors acknowledge the support of CASR, BUET for this research.

## Nomenclature

$a$	– amplitude, [m]
$D_h$	– hydraulic diameter ( $H_{\min} + H_{\max}$ ), [m]
$f$	– friction factor per wave length, [–]
$H$	– height of the channel, [m]
$h$	– convective heat transfer coefficient, [ $\text{Wm}^{-2}\text{K}^{-1}$ ]
$\kappa$	– thermal conductivity, [ $\text{Wm}^{-1}\text{K}^{-1}$ ]
Nu	– Nusselt number, [ $hD_h/k$ ]
$p$	– pressure, [Pa]
Re	– Reynolds number, [ $=u_{\text{avg in}}H_{\min}/\nu$ ], [–]
$T$	– temperature, [K]
$T_b$	– bulk mean temperature, [K]
$t$	– time, [s]
$u$	– X component of velocity, [ $\text{ms}^{-1}$ ]
$u_{\text{avg}}$	– mean velocity, [ $\text{ms}^{-1}$ ]
$v$	– Y component of velocity, [ $\text{ms}^{-1}$ ]

### Greek symbols

$\alpha$	– thermal diffusivity, [ $\text{Wm}^{-2}\text{K}^{-1}$ ]
$\theta$	– dimensionless temperature, $(T - T_w)/(T_{\text{bin}} - T_w)$ , [–]
$\lambda$	– wavelength, [m]
$\mu$	– viscosity, [ $\text{Nsm}^{-1}$ ]
$\nu$	– kinematic viscosity, [ $\text{m}^2\text{s}^{-1}$ ]
$\rho$	– density of fluid, [ $\text{kgm}^{-3}$ ]

### Subscripts

avg	– average
in	– value at inlet
max	– maximum value
min	– minimum value
w	– value at wall

## References

- [1] Nishimura, T., Ohori, Y., Kawamura, Y., Flow Characteristics in a Channel with Symmetric Wavy Wall for Steady Flow, *J. Chem. Engg. Japan*, 17 (1984), 5, pp. 466-471
- [2] Sparrow, E. M., Comb, J. W., Effect of Interwall Spacing and Fluid Flow Inlet Conditions on a Corrugated-Wall Heat Exchanger, *Int. J. Heat Mass Transfer*, 26 (1983), 7, pp. 993-1005
- [3] Sparrow, E. M., Hossfeld, L. M., Effect of Protruding Edges on Heat Transfer and Pressure Drop in Duct, *Int. J. Heat Mass Transfer*, 27 (1984), 10, pp. 1715-1722
- [4] Wang, G., Vanka, S. P., Convective Heat Transfer in Periodic Wavy Passages, *Int. J. Heat Mass Transfer*, 38 (1995), 17, pp. 3219-3230
- [5] Stone, K., Vanka, S. P., Numerical Study of Developing Flow and Heat Transfer in a Wavy Passage, *Journal of Fluids Engineering* (Transactions of ASME), 121 (1999), 4, pp. 713-719
- [6] Niceno, B., Nobile, E., Numerical Analysis of Fluid Flow and Heat Transfer in Periodic Wavy Channels, *International Journal of Heat and Fluid Flow*, 22 (2001), 2, pp. 156-167
- [7] Ferziger, J., Peric, M., Computational Methods for Fluid Dynamics, Springer Verlag, Berlin, Heidelberg, 1996
- [8] Hossain, M. Z., Numerical Investigation of Unsteady Flow and Heat Transfer in Wavy Channels, M. Sc. Eng. thesis, Department of Mechanical Engineering, Bangladesh University of Engineering and Technology (BUET), Dhaka, 2003

Authors' addresses:

*M. Z. Hossain*

Department of Mechanical & Materials Engineering,  
The University of Western Ontario  
London, Ontario, Canada, N6A 5B9

*A. K. M. Sadrul Islam*

Mechanical & Chemical Engineering Department,  
Islamic University of Technology,  
The Organization of the Islamic Conference  
Board Bazar, Gazipur 1704, Bangladesh

Corresponding author A. K. M. Sadrul Islam

E-mail: sadrul@iut-dhaka.edu, sadrul@me.buet.ac.bd

Paper submitted: March 13, 2006  
Paper revised: November 25, 2006  
Paper accepted: November 29, 2006